New Journal of Physics
The open access journal at the forefront of physics

Deutsche Physikalische Gesellschaft DPG IOP Institute of Physics

PAPER • OPEN ACCESS

Structure and electronic states of vicinal Ag(111) surfaces with densely kinked steps

To cite this article: J Enrique Ortega *et al* 2018 *New J. Phys.* **20** 073010

New Journal of Physics
The open access journal at the forefront of physics

Deutsche Physikalische Gesellschaft DPG
IOP Institute of Physics

Published in partnership with: Deutsche Physikalische Gesellschaft and the Institute of Physics

OPEN ACCESS

RECEIVED
31 March 2018

REVISED
4 June 2018

ACCEPTED FOR PUBLICATION
11 June 2018

PUBLISHED
4 July 2018

PAPER

Structure and electronic states of vicinal Ag(111) surfaces with densely kinked steps

J Enrique Ortega[1,2,3], Guillaume Vasseur[3], Ignacio Piquero-Zulaica[2], Sonia Matencio[4], Miguel Angel Valbuena[4], Julien E Rault[5], Frederik Schiller[2], Martina Corso[2], Aitor Mugarza[4,6] and Jorge Lobo-Checa[7,8]

[1] Departamento Física Aplicada I, Universidad del País Vasco, E-20018-San Sebastian, Spain
[2] Centro de Física de Materiales CSIC/UPV-EHU-Materials Physics Center, Manuel Lardizabal 5, E-20018-San Sebastian, Spain
[3] Donostia International Physics Centre, Manuel Lardizabal 5, E-20018-San Sebastian, Spain
[4] Catalan Institute of Nanoscience and Nanotechnology (ICN2), CSIC and The Barcelona Institute of Science and Technology, Campus UAB, Bellaterra, E-08193 Barcelona, Spain
[5] Synchrotron SOLEIL, L'Orme des Merisiers Saint-Aubin, BP 48 F-91192 Gif-sur-Yvette Cedex, France
[6] ICREA, Institució Catalana de Recerca i Estudis Avançats, Lluis Companys 23, E-08010 Barcelona, Spain
[7] Instituto de Ciencia de Materiales de Aragón (ICMA), CSIC-Universidad de Zaragoza, E-50009 Zaragoza, Spain
[8] Departamento de Física de la Materia Condensada, Universidad de Zaragoza, E-50009 Zaragoza, Spain

E-mail: enrique.ortega@ehu.es

Keywords: vicinal surface, curved surface, kinked step, STM, photoemission, surface states, Ag(111)

Supplementary material for this article is available online

Abstract

Vicinal surfaces exhibiting arrays of atomic steps are frequently investigated due to their diverse physical-chemical properties and their use as growth templates. However, surfaces featuring steps with a large number of low-coordinated kink-atoms have been widely ignored, despite their higher potential for chemistry and catalysis. Here, the equilibrium structure and the electronic states of vicinal Ag(111) surfaces with densely kinked steps are investigated in a systematic way using a curved crystal. With scanning tunneling microscopy we observe an exceptional structural homogeneity of this class of vicinals, reflected in the smooth probability distribution of terrace sizes at all vicinal angles. This allows us to observe, first, a subtle evolution of the terrace-size distribution as a function of the terrace-width that challenges statistical models of step lattices, and second, lattice fluctuations around resonant modes of surface states. As shown in angle resolved photoemission experiments, surface states undergo stronger scattering by fully-kinked step-edges, which triggers the full depletion of the two-dimensional band at surfaces with relatively small vicinal angles.

Introduction

Vicinal surfaces are important in catalysis, nanostructure growth, or electronic state engineering, since steps are active sites for chemical reactions, as well as nucleation and electron scattering centers. Note that the random truncation of the crystalline solid will generally result in a surface plane that is tilted with respect to a high-symmetry direction, namely in a vicinal surface. Therefore, vicinal surfaces are more 'abundant' than high-symmetry surfaces, and this may have particular impact, e.g., in the physical-chemistry of nano-sized particles, which expose all crystal orientations [1, 2]. However, given the infinite possibilities for vicinal surface planes, it is therefore important to perform their systematic investigation, in order to appropriately determine key magnitudes and parameters that govern specific phenomena, and to facilitate the selection of optimal substrates for desired functions.

During the last decade, a number of studies have been aimed at systematically exploring vicinal surfaces using crystal samples with both spherical and cylindrical shapes, mostly metals [3–9], but also semiconductors [10]. Using such samples one can probe entire families of vicinal planes, and hence provide a comprehensive understanding of all physical-chemical properties connected to the presence of surface steps. In fact, the ability

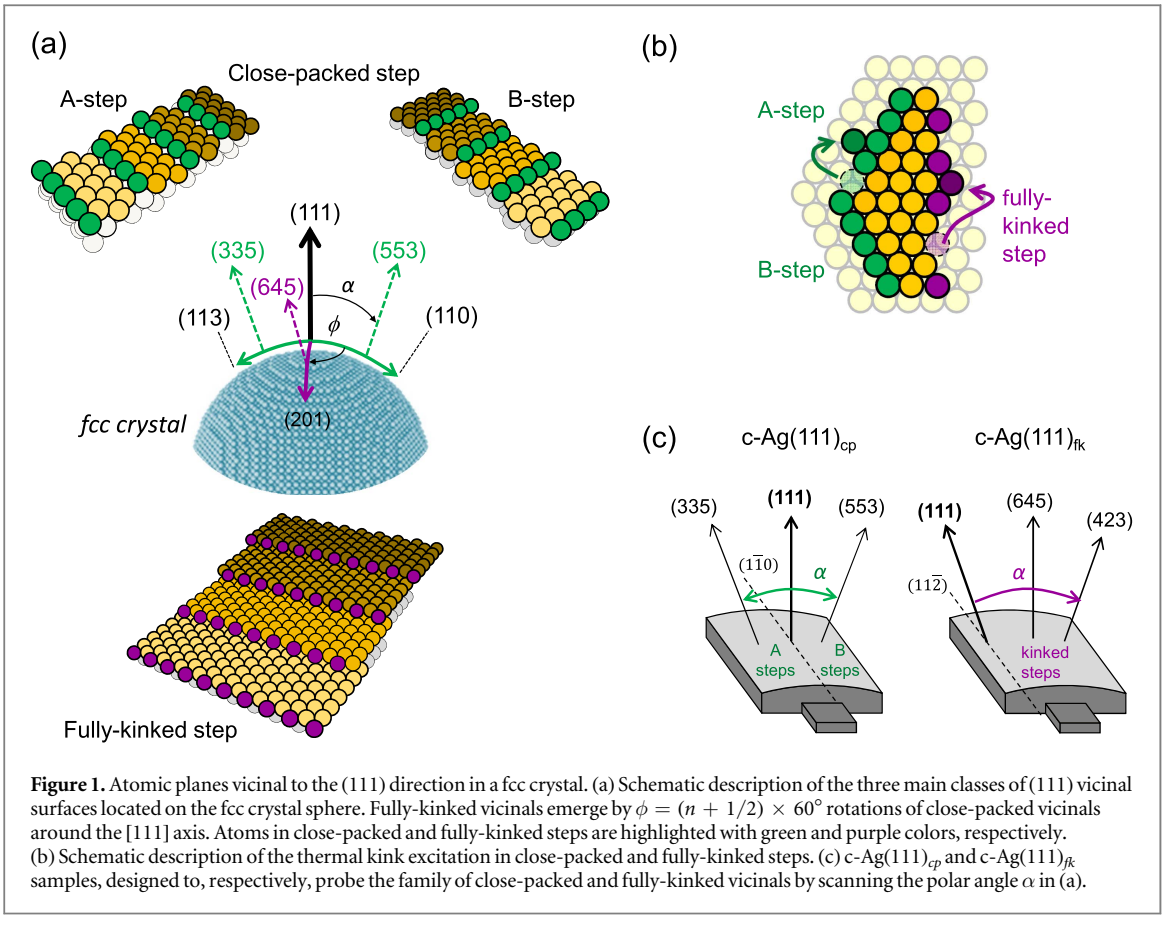

Figure 1. Atomic planes vicinal to the (111) direction in a fcc crystal. (a) Schematic description of the three main classes of (111) vicinal surfaces located on the fcc crystal sphere. Fully-kinked vicinals emerge by $\phi = (n + 1/2) \times 60°$ rotations of close-packed vicinals around the [111] axis. Atoms in close-packed and fully-kinked steps are highlighted with green and purple colors, respectively. (b) Schematic description of the thermal kink excitation in close-packed and fully-kinked steps. (c) c-Ag(111)$_{cp}$ and c-Ag(111)$_{fk}$ samples, designed to, respectively, probe the family of close-packed and fully-kinked vicinals by scanning the polar angle α in (a).

to compare a high-symmetry surface with its vicinal stepped planes on the same sample has been proved essential to clarify controversial issues, such as the quantum-mechanical nature of surface electronic states away from the high-symmetry plane [4, 11], or to unveil new general properties, such as structural transitions and fluctuations of the surface as a function of the vicinal angle α [3, 4, 7–9]. The latter is particularly important, due to its direct connection with the equilibrium shape of three-dimensional nanocrystals, but also attractive from a fundamental point of view, since a vicinal surface can be regarded as a superlattice of steps subject to thermal disorder, equivalent to a one-dimensional (1D) gas of fermions [12–15]. In this context, complete, α-dependent terrace-width distribution data sets, such as those that can systematically be acquired from curved surfaces, are highly desired to test and further refine theoretical statistical physics models and concepts for step lattices.

In this work we follow the curved surface approach to investigate structural and electronic properties of vicinal Ag(111) surfaces featuring fully-kinked steps. In general, vicinal (111) surfaces of fcc crystals are chosen to exhibit steps with close-packed configuration (oriented along the [1-10] direction), whereas vicinals with fully-kinked steps (oriented along the [1-12] direction, and also called 100% kinked [16]) have been very scarcely studied. This is striking, since due to the lower atomic coordination of such kinks these surfaces are particularly attractive to investigate chemical reactions and catalysis [17]. Here we show that this class of vicinals offers a better definition of the terrace-width distribution obtained from scanning tunneling microscopy (STM) image analysis. This allowed us to observe a striking transition from sharply defined step lattices for high step densities, to much broader arrays at low densities that exhibit well-defined modulations due to electronic effects. On the other hand, angle resolved photoemission (ARPES) experiments demonstrate a relatively strong scattering of the Shockley state in vicinal planes, which results in a complete depletion of the surface band due to terrace (lateral) confinement effects. The strong scattering amplitude is in agreement with the observation of electronic quantum size effects.

Cylindrical section approach to study vicinal surfaces

The fcc crystal sphere in figure 1(a) allows us to locate different vicinal directions and types of steps. The high-symmetry (111) plane is placed at the north pole, whereas surfaces with increasing vicinal angle α are found following meridian directions. The azimuthal angle ϕ defines the type of step, which can be close-packed A type ({100}-like minifacet) at $\phi = 180°$ (green meridian), close-packed B type ({111}-like minifacet) at $\phi = 0°$

(green meridian), or fully-kinked at $\phi = 90^\circ$ (purple meridian). As a way of example, the atomic structure for the A type (335), the B type (553), and the fully-kinked (645) planes are shown in figure 1(a). The most important difference among them is the coordination of the outermost step-edge atoms, which is sevenfold for the close-packed arrangement (either A or B) and sixfold for the fully-kinked case. Chiral vicinal surfaces, defined by sevenfold close-packed step segments separated by sixfold-coordinated kinks are found at ϕ values other than $\phi = n \times 30^\circ$, although these are not discussed in the present work. As indicated in figure 1(a), one may consider that the (111) 'vicinality' ends at the (110) ($\phi = 0^\circ$, $\alpha = 35^\circ$), (113) ($\phi = 180^\circ$, $\alpha = 29^\circ$) and (201) ($\phi = 90^\circ$, $\alpha = 39^\circ$) planes, at which no ninefold-coordinated atoms, i.e., (111) terraces remain.

The different coordination of close-packed and fully-kinked steps has a direct implication in the excitation of step-edge atoms, usually called 'thermal kinks', as sketched in figure 1(b). Atoms excited-out and diffusing-along step-edges represent the lowest energy atomic excitation (lowest number of broken bonds) at a crystal surface, and are essential to explain the equilibrium structure of vicinal planes [15]. In this respect, the energy path to create thermal kinks is radically different in each case. For the sevenfold coordinated atom embedded in the close-packed step (either A or B) one needs to break four surface bonds to move this atom to a five-fold neighbor site (green arrow). In the fully-kinked step, exciting the kink atom requires breaking three surface bonds, although moving such atom to a new step-edge position does not change its sixfold atomic coordination (red arrow). This implies that fully-kinked surface steps can roughen or 'bend' at a local scale in a rapid process (smaller number of broken bonds) and without energy penalty (same coordination at new step-edge site), leading to faster step diffusion kinetics (also called step meandering). As we shall see below, this explains why fully-kinked vicinal surfaces exhibit strong and fast step fluctuations at 300 K, bringing them closer than close-packed vicinals to its equilibrium structure.

By taking cylindrical sections along meridian lines of figure 1(a) one can systematically test vicinal planes of the fcc crystal sphere [18]. For a given sample, we fix the type of step (constant ϕ) and allow the step density to change smoothly (variable α). We choose a convenient geometry and size (radius of curvature) to facilitate processing in vacuum, and selective testing of the different vicinal planes by ARPES, for which sufficiently small, <100 μm photon beams must be used (see supplementary information, available online at stacks.iop.org/NJP/20/073010/mmedia). Here we focus on the sample described as c-Ag(111)$_{fk}$ in figure 1(c) to investigate the basic structural and electronic properties of fully-kinked vicinal surfaces, but also compare the results with those obtained in close-packed Ag(111) vicinals, studied in [4, 11] using the sample named as c-Ag(111)$_{cp}$ in figure 1(c). This comparative analysis is extensively presented in the SI.

Terrace-width distribution: step lattice models and electronic fluctuations

The STM pictures of figures 2(a) and (b) have been selected to illustrate the characteristic nanoscale morphology of a fully-kinked Ag(111) vicinal surface at 300 K in two different cases, namely surfaces with large ($\alpha = 12^\circ$) and small ($\alpha = 1.3^\circ$) vicinal angles. The complete set of STM data is presented and discussed in the SI. As previously observed in STM experiments at 300 K [4, 19], monatomic steps in Ag(111) look frizzy due to the presence of thermally-excited kinks and out-protruding fringes induced by the STM tip. The morphology of the step-edge is better observed in the inset of figure 2(a), which shows a portion of the image after derivation and smoothing. This process removes the tip-induced fringes, allowing a precise observation of the wavy structure of the step-edge. The latter is further discussed and analyzed in the SI. Importantly, step fluctuations cause the local variation of the terrace-width d around its mean value $<d> = h/\sin\alpha$ (where $h = 2.35$ Å is the monatomic step height). $\langle d \rangle$ is statistically determined from the probability distribution of terrace sizes $P(s)$ in each image, represented in figure 2(c). To better compare both we use the reduced terrace-width coordinate $s = d/\langle d \rangle$, and normalize curves to the maximum probability value. Here we see the large differences between $P(s)$ histograms at the two different step density regimes. At the small $\langle d \rangle = 1.13$ nm ($\alpha = 12^\circ$) step lattice periodicity, $P(s)$ looks sharp and symmetric, while for $\langle d \rangle = 10.2$ nm ($\alpha = 1.3^\circ$) $P(s)$ becomes broad and asymmetric.

The terrace-width probability has been obtained for a whole set of STM images acquired across the surface (see SI), and the result is represented in figure 2(c) as a $P(s)$ intensity plot. For small $\langle d \rangle$ one can observe the sharp and symmetric $P(s)$ histograms peaking close to $s = 1$ ($d =$). By increasing $\langle d \rangle$, the $P(s)$ maximum progressively shifts to the left side, whereas probability fluctuations develop in the right side tail. As indicated in the figure and discussed in the next section, such evolution of $P(s)$ reflects the progressive damping of the elastic step repulsion that holds the periodic structure of the vicinal surface [12, 13, 15], giving rise to the emergence of electronic-energy driven fluctuations at large terrace widths [14].

The accurate analysis of $P(s)$ is of major importance to understand the mechanisms underlying the equilibrium structure of a vicinal surface [12, 13, 15]. Over the past thirty years, the continuum theory, represented by the surface free energy equation as a function of the vicinal angle $\sin\alpha = h/d$ [12], combined with different statistical physics models have been used to explain experimental $P(s)$ data (see [13, 14] and

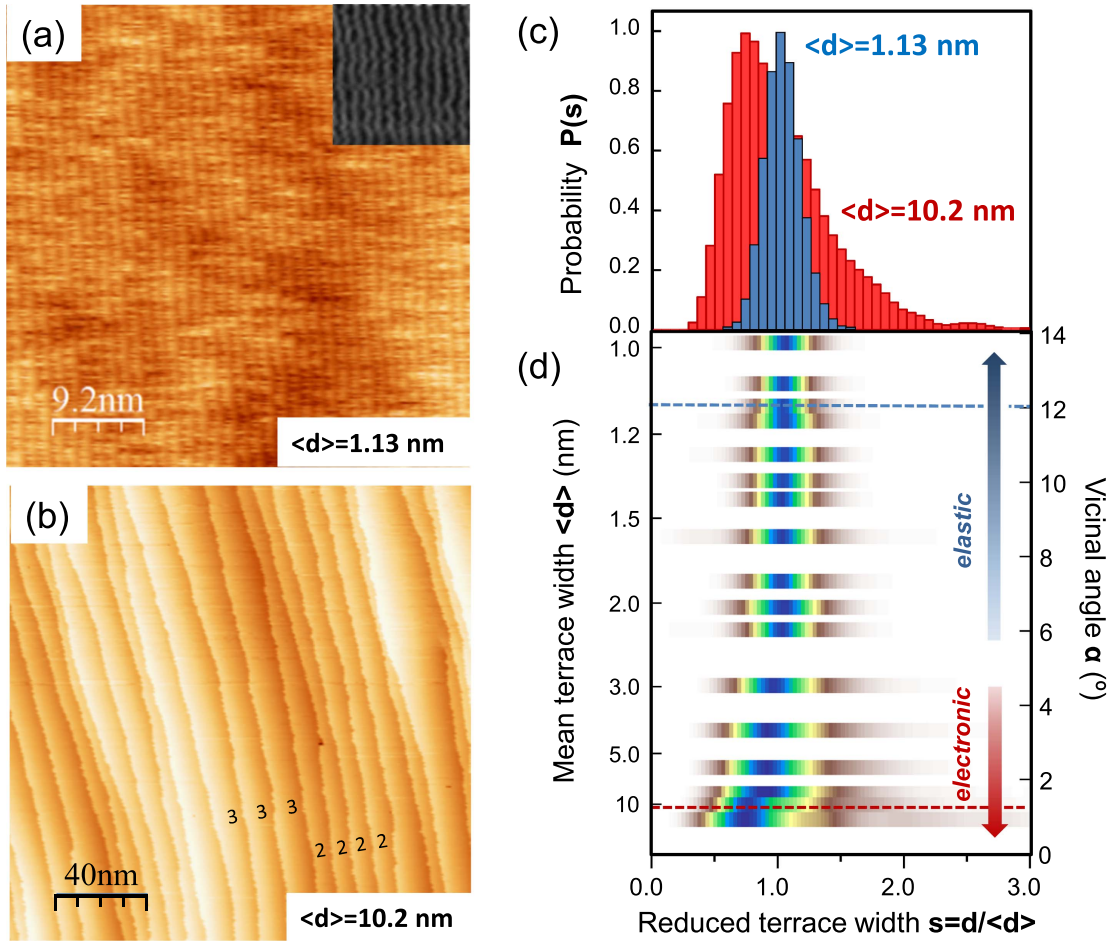

Figure 2. Terrace-width probability analysis of the curved Ag crystal with fully-kinked steps. STM images taken at 300 K on the c-Ag(111)$_{fk}$ sample at (a) $\alpha = 12°$ and (b) $\alpha = 1.3°$ vicinal angles. The indicated $\langle d \rangle$ values are determined from the corresponding statistical analysis of the terrace-width histograms $P(d)$ shown in (c). The inset in (a) shows a portion of the image after derivation and smoothing, reflecting the rough morphology of the step (see SI for a discussion). The numbers n in (b) mark magic d_n sizes due to electronic instabilities (see figure 3). (d) $P(d/\langle d \rangle)$ probability histograms from the full set of STM images taken across the c-Ag(111)$_{fk}$ sample (see SI).

references therein). Among such models, the most successful one is the so-called terrace-step-kink (TSK) [15]. In the TSK model steps are allowed to meander through the thermal excitation of kinks, although free meandering is constrained by the elastic repulsion between neighboring steps, simplified in a single force-dipole term, and by the entropic 'repulsion', namely the restriction set by non-crossing conditions of contiguous steps. Both entropic and elastic step interactions are accounted for in the second order ($1/d^2$) term of the surface free energy equation [12]. On the grounds of the TSK approach, one can find (or 'surmise') an elegant expression for the equilibrium shape $P(s)$ of the vicinal surface called 'generalized Wigner-surmise' (GWS) [15]. The GWS function for the terrace-width probability can be written as a function of the reduced coordinate $s = d/\langle d \rangle$ and the order parameter ϱ as:

$$P_\varrho(s) = a_\varrho s^\varrho \mathrm{e}^{-b_\varrho s^2}, \tag{1}$$

where b_ϱ fixes the mean of $P_\varrho(s)$ at $s = 1$, and a_ϱ normalizes the total probability $\int_0^\infty P_\varrho(s)\,\mathrm{d}s = 1$. In reality, ϱ is intimately linked to a dimensionless step interaction parameter $\tilde{A}$, through the expression $\varrho = 1 + \sqrt{1 + 4\tilde{A}}$ [15]. $\tilde{A}$ is a meaningful magnitude that quantifies the elastic/entropic interaction ratio as $\tilde{A} = A\tilde{\beta}/k_B T$, where A is the dipole interaction strength between contiguous steps and $\tilde{\beta}$ the step stiffness [15].

The ability of experimentally testing the GWS solution of equation (1) has been rather limited so far. The reason is the lack of statistically reliable $P(s)$ data sets, which makes it impossible to discriminate among $P_\varrho(s)$ functions of different order parameter ϱ. In the present case, the systematics of the curved surface and the high-quality of the $P(s)$ data for fully-kinked vicinals (also compared to close-packed surfaces, see SI), allows us to perform such a test. In figure 3(a) the experimental $P(s)$ histograms have been fitted with $P_\varrho(s)$ functions (lines), using ϱ as the single fitting parameter. Histograms for densely stepped surfaces with $\langle d \rangle$ below 3.0 nm fit to GWS functions excellently, leading to the linear ϱ variation (blue region) shown in figure 3(b). This ϱ variation

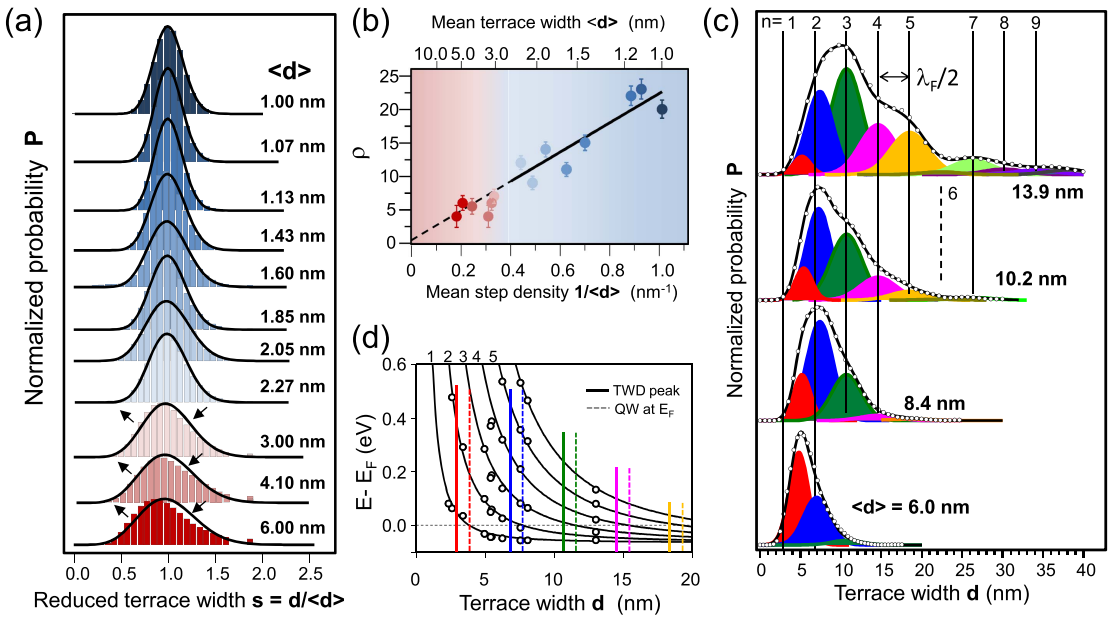

Figure 3. Analysis of the elastic and electronic instability regimes. (a) Fit (thick lines) of probability histograms $P(d/\langle d\rangle)$ of the c-Ag(111)$_{fk}$ sample with GWS functions of variable order parameter ϱ. The resulting ϱ values are plotted in panel (b). Blue data correspond to GWS fits with negligible standard deviation, and have been fitted with a straight line. Red data correspond to the histograms in (a) where the fit visually departs from data (as marked with arrows, other data are also included). (c) $P(d)$ data for large $\langle d\rangle$, fitted with a single series of Gaussian functions, of increasing width and variable intensity. Gaussian positions lie close to expected multiples of quantum well resonances at E_F, defined as $d_n = n \times \lambda_F/2 - d_0$ (vertical lines). (d) n-quantum well resonances measured in scanning tunneling spectroscopy (STS) in Ag(111) terraces of different d sizes (see SI). Lines fit the n-sets of data assuming a nearly-free-electron model (see [20]). These lines cross E_F at d values indicated by the thin dotted vertical lines. Thick solid vertical lines mark the d_n series of gaussians of panel (c).

indicates that the balance of elastic and entropic interactions, represented by $\tilde{A}$, is changing as a function of $\langle d\rangle$. Although it appears reasonable to expect strong elastic repulsion for small step spacings, and vanishing elastic interactions between steps for large step-step separations, the d-dependence of $\tilde{A}$ cannot be deduced from the standard TSK model and the continuum approach, where the dipole strength A and the step stiffness $\tilde{\beta}$ are assumed as constants. The necessity of a variable ϱ to consistently fit the $P(s)$ data of figure 3(a) thus reflects the limited validity of the force-dipole approach, which restricts elastic interactions between steps to the second order term (A/d^2) in the free energy equation [12].

As indicated by the arrows in figure 3(a), the $P(s)_\varrho$ fit to the STM histograms begins to fail at $\langle d\rangle = 3.0$ nm, while above $\langle d\rangle = 6.0$ nm the GWS solution breaks down clearly. The resulting ϱ values in the $\langle d\rangle = 3.0$–6.0 nm range were also included in figure 3(b) as red data points, but not taken into account for the linear fit. The $P(d)$ probability histograms for step lattices with $\langle d\rangle$ above 6.0 nm are depicted in figure 3(c) using circular markers. The asymetric broadening of the curves increases dramatically when comparing to the sharply-peaked histograms of panel figure 3(a). This drastic change in the shape of $P(d)$ is common to other metal surfaces [7, 8], but only in the present case the smooth histograms of figure 3(c) allow the observation of fine modulations on the right hand tail that can be fitted with a set of Gaussian functions, which suggest the presence of terrace-width fluctuations around preferred (or 'magic') d_n values.

At vicinal noble metal surfaces one can reasonably expect magic d_n sizes matching 1D quantum well (QW) resonances of surface electrons confined within terraces, as discussed by Ibach [14]. In fact, the Shockley state carries a sizeable charge, sufficient to trigger 1D-charge-density-wave instabilities in step arrays via Fermi surface nesting and gap opening [21]. Such structural/electronic interplay was indeed invoked to explain the fluctuations of $P(d)$ observed on c-Cu(111) at $\langle d\rangle$ values around half the Fermi wavelength $\lambda_F/2 \sim 2$ nm [4]. In that surface, though, the $P(d)$ histogram did not show clear shoulders as in figure 3(c), but a strong width fluctuation around $\lambda_F/2$. To test the electronic origin of the modulations observed in the $P(d)$ in the large terrace regime, in figure 3(c) we compare the positions of the multiple Gaussians obtained in the fit with $d_n = n \times \lambda_F/2 - d_0$, a set of vertical lines spaced by half-multiples of the Fermi wavelength and offset by d_0 ($\lambda_F/2 = 3.9$ nm in Ag(111) [22]). The match between peaks and lines is excellent for $d_0 = 1$ nm, except for $n = 1$. The latter is indeed expected, since step fluctuations towards low d values are effectively blocked by the elastic and entropic step-step repulsions.

The presence of QW resonances in Ag(111) terraces can be readily proven in scanning tunneling spectroscopy (STS) measurements (see for example [20, 22, 23] and SI). Their localization at E_F can be predicted

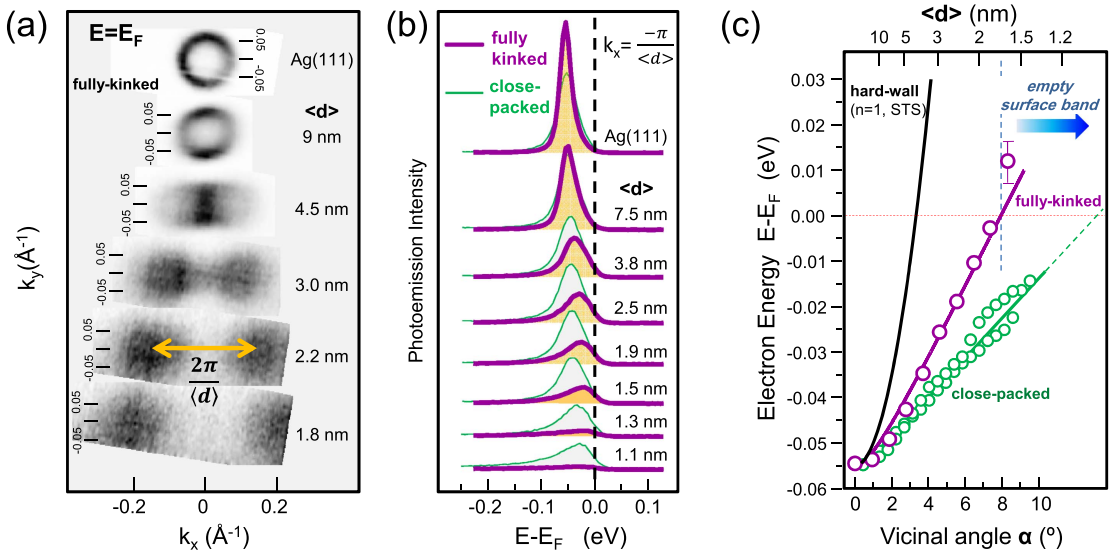

Figure 4. Surface states at fully-kinked Ag(111) vicinal surfaces. (a) Constant energy surface at the Fermi energy acquired across the c-Ag(111)$_{fk}$ sample, exhibiting $2\pi/\langle d\rangle$ Shockley umklapps of the step superlattice (Photon energy $h\nu = 41$ eV, $T = 100$ K). (b) Energy distribution curves at Shockley band minima ($k_x = \pi/\langle d\rangle$) across the fully-kinked c-Ag(111)$_{fk}$ surface (purple thick lines), compared to the band minima at the close-packed c-Ag(111)$_{cp}$ sample (green thin lines, from [4]). (c) Shockley band minimum energy as a function of the vicinal angle α for fully-kinked (purple dots) and close-packed (A and B, green dots), fitted with a 1D Kronig–Penney model (lines) [4], which, respectively, renders a scattering barrier strength ($V_0 \times b$) of 1.1 eV Å and 0.6 eV Å. The relatively large $V_0 \times b$ value for the fully-kinked step leads to the full depletion of the surface band for $d < 1.7$ nm. The solid black line indicates the energy of the $n = 1$ QW state ($n = 1$ fitting line in figure 3(d)). Experiments have been performed at the Casiopee beam line in Soleil synchrotron.

from the whole terrace-width dependent analysis of such resonances, such as the one shown in figure 3(d).[9] Here circular markers indicate the peak energies of the n-QW resonance measured in STS spectra (see SI and [11, 20]), whereas solid lines fit each QW set of points with a nearly-free electron model, based on the parabolic fit to the surface band dispersion directly probed in STS [11]. The successive crossing points of these lines at E_F appear marked with vertical dotted lines in figure 3(d), defining d_n^* values at which the density of states at E_F is maximum. These can be compared with the $d_n = n \times \lambda_F/2 - d_0$ series of figure 3(c). We observe that, excluding d_1, and due to the d_0 shift, magic d_n sizes of figure 3(c) appear right below d_n^* terraces with electron density maxima at E_F. This means that for the n-magic size the n-QW resonance lies right above E_F, which in fact corresponds to a periodic minimum in a d-dependent electronic-energy.

Step barrier strength and depletion of the surface band

Confinement of surface electrons in terraces occurs because atomic steps act as repulsive barriers for surface states, such as Shockley states in Ag(111) [19, 22]. ARPES can also be used to test surface electron scattering in arrays of steps at vicinal surfaces [4]. Early experiments have shown the existence of zone-boundary gaps and umklapps, which prove the presence of weak scattering of the 2D Shockley state by the periodic step potential. Such coherent 2D surface band has been seldom detected in STS experiments from step arrays [24], since its emission is largely obscured by the presence of strong 1D QW resonances confined within random, individual (111) terraces (see SI and [20]). Conversely, QW resonances are only detectable in ARPES in highly disordered step lattices, through careful inspection of three-dimensional Fourier maps [11, 25]. Weak periodic potential effects also appear in ARPES experiments performed on fully-kinked Ag(111) vicinals, as shown in figure 4(a). The 2D Fermi intensity measured across the curved c-Ag(111)$_{fk}$ sample exhibits the characteristic Ag(111) Fermi surface ring split by $k_x = 2\pi/\langle d\rangle$ superlattice wavevectors. The ring radius shrinks and its intensity weakens as the mean terrace-size $\langle d\rangle$ decreases, due to the repulsive character of the step potential and the subsequent upward shift of the Shockley band. Such terrace-size effect is better observed in figure 4(b), where we plot energy distribution curves (EDC) corresponding to the Shockley band minimum at $k_x = \pi/\langle d\rangle$ across the c-Ag(111)$_{fk}$ surface. Data are compared to EDC-s acquired at equivalent $\langle d\rangle$ values on the c-Ag(111)$_{cp}$ surface. As $\langle d\rangle$ progressively decreases, the EDC spectrum shifts to higher energy, and eventually crosses the Fermi level. This process is notably faster for the fully-kinked vicinals, that is, the step potential is stronger compared to that of the

[9] The quantum well resonances of figure 3(d) have been measured on a Ag(111) vicinal surface with close-packed steps, but the Fermi level crossing of resonances is not expected to depend on the step type.

close-packed vicinals. Note that at small $\langle d \rangle$ values a clear Fermi-edge like spectrum is observed, meaning that the surface band is totally depleted.

The strength of the step potential can be estimated from the terrace-size shift of figure 4(b), assuming a 1D Kronig–Penney model of the step lattice [4]. This is the simplest crystal potential one can think of, which is defined by a periodic series (period d) of square barriers (barrier height V_0, width b) in one dimension. The result is shown in figure 4(c) for fully-kinked vicinals, and compared to close-packed vicinals (A and B type, see [4]). We also plot the expected shift for an infinite, hard-wall potential, namely for the $n = 1$ QW state, which is the main spectral feature detected in STS at Ag(111) terraces of random size d (see [19, 20] and figure 3(d)). Data points are determined from the EDC spectra of figure 4(b), which were fitted with the standard gaussian-broadened Lorentzian line, convoluted with a Fermi-edge [4]. Using the periodic potential strength $V_0 \times b$ as unique input parameter, the Kronig–Penney fit leads to $V_0 \times b = 0.6$ eV Å for close-packed, and $V_0 \times b = 1.1$ eV Å for fully-kinked Ag steps. The scattering potential of the atomic step is believed to be linked to the so-called Smoluchowski dipole that arises at step-edge atoms [26], which is generally larger for atoms with lower coordination at kink sites, compared to atoms at close-packed steps [27]. Alternatively, the larger $V_0 \times b$ barrier in the fully-kinked step-edge could also reflect its structural relaxation into close-packed zigzag segments, which defines an effectively longer close-packed step length (see SI).

Due to the large terrace-size effect, the Shockley band in fully-kinked vicinals shifts above E_F for step lattice periodicity $\langle d \rangle$ below 1.7 nm (vicinal angles larger than $\alpha = 8°$), as indicated in figure 4(c). This is a peculiar situation, in which the vicinal surface would be completely depleted of 2D surface electrons with relatively large d values. 2D Shockley band depopulation of Ag(111) has also been observed in thin Ag(111) films submitted to large elastic strain [28]. For close-packed vicinals, the extrapolation of the Kronig–Penney fit indicates that depopulation of the 2D electron band occurs for d below 1 nm (above $\alpha = 16°$). In contrast, depopulation of 1D QW electrons trapped at random Ag(111) terraces has already occurred at $d < 3.2$ nm, as marked by the EF crossing of the thick black line (see also [19, 20] and figure 3(d)), which corresponds to a vicinal surface with less than two rows of (111) terrace atoms, namely a surface with dominant step sites. The influence of surface electrons confined at local defects, is well known, for example, in the chemical activity of nanocrystals [2]. But its importance is not clear for extended states, such as Shockley states, whose real impact in the physical-chemistry of noble metal surfaces remained merely speculative [29]. In this sense, we believe that curved noble metal surfaces offer the appropriate platform to revisit this key surface property.

Conclusions

In summary, following the curved surface approach we have investigated the equilibrium structure of the step lattice and the scattering of the Shockley state in vicinal Ag(111) surfaces with fully-kinked steps as a function of the step density. Through the terrace-width distribution analysis performed with STM we are able to track the transition from sharply defined step lattices for high step densities to broader distributions at low densities, which, respectively, define regimes dominated by elastic step interactions and quantum electronic effects. The terrace-width distribution for the high step density regime is very well described through the GWS function derived from the TSK model, but only when assuming a variable balance of entropic and elastic interactions, which the current TSK model does not contemplate. This finding underlines the limits of the standard three-term, free energy equation derived in the elastic continuum approach used to describe a vicinal surface. In the low step density regime, we additionally observe terrace-width distribution fluctuations, which are related to the quantization of the Shockley surface states due to confinement between adjacent steps. In fact, the TWD peaks follow the same periodicity of the Fermi level crossing of the QW resonances, in analogy to the quantum size effects observed in the thickness stability of 2D films. In ARPES we observe a rapid upward shift of the surface band as a function of the step density, which causes its complete depletion at a relatively small vicinal angle. This effect arises due to the large scattering strength of the fully-kinked step, as compared to that of the close-packed step.

Acknowledgments

We acknowledge Bihurcrystal Ltd. for providing a prototype fully-kinked Ag curved crystal sample. We are grateful to the CASIOPEE beam line staff at the SOLEIL Synchrotron in France. We acknowledge the financial support from the Spanish Ministry of Economy, Industry and Competitiveness (MINECO, Grant No. MAT2016-78293-C6 and Severo Ochoa No. SEV-2013-0295), the Basque Government (Grant No. IT-621-13), the regional Government of Aragon (RASMIA project), the CERCA Programme/Generalitat de Catalunya, and the European Regional Development Fund (ERDF) under the program Interreg V-A España-Francia-Andorra

(Contract No. EFA194/16 TNSI). Very enriching discussions with Professor Theodore Einstein are gratefully acknowledged.

ORCID iDs

Frederik Schiller https://orcid.org/0000-0003-1727-3542
Aitor Mugarza https://orcid.org/0000-0002-2698-885X

References

[1] Somorjai G and Li Y 2010 *Introduction to Surface Chemistry and Catalysis* (New York: Wiley)
[2] Boles M A, Ling D, Hyeon T and Talapin D V 2016 The surface science of nanocrystals *Nat. Mater.* **15** 141
[3] Corso M, Schiller F, Fernández L, Cordón J and Ortega J E 2009 Electronic states in faceted Au(111) studied with curved crystal surfaces *J. Phys.: Condens. Matter* **21** 353001
[4] Ortega J E, Corso M, Abd-el Fattah Z M, Goiri E A and Schiller F 2011 Interplay between structure and electronic states in step arrays explored with curved surfaces *Phys. Rev.* B **83** 085411
[5] Mom R V, Hahn C, Jacobse L and Juurlink L B 2013 LEED analysis of a nickel cylindrical single crystal *Surf. Sci.* **613** 15–20
[6] de Alwis A, Holsclaw B, Pushkarev V, Reinicker A, Lawton T, Blecher M, Sykes E and Gellman A 2013 Surface structure spread single crystals (S4C): preparation and characterization *Surf. Sci.* **608** 80–7
[7] Walter A L *et al* 2015 X-ray photoemission analysis of clean and carbon monoxide-chemisorbed platinum(111) stepped surfaces using a curved crystal *Nat. Commun.* **6** 8903
[8] Ilyn M, Magaña A, Walter A L, Lobo-Checa J, de Oteyza D G, Schiller F and Ortega J E 2017 Step-doubling at vicinal Ni(111) surfaces investigated with a curved crystal *J. Phys. Chem.* C **121** 3880–6
[9] Blomberg S *et al* 2017 Strain dependent light-off temperature in catalysis revealed by planar laser-induced fluorescence *ACS Catal.* **7** 110–4
[10] Miccio L A *et al* 2016 Interplay between steps and oxygen vacancies on curved TiO_2(110) *Nano Lett.* **16** 2017–22
[11] Ortega J E, Lobo-Checa J, Peschel G, Schirone S, Abd El-Fattah Z M, Matena M, Schiller F, Borghetti P, Gambardella P and Mugarza A 2013 Scattering of surface electrons by isolated steps versus periodic step arrays *Phys. Rev.* B **87** 115425
[12] Williams E D and Bartelt N C 1991 Thermodynamics of surface morphology *Science* **251** 393–400
[13] Jeong H-C and Williams E D 1999 Steps on surfaces: experiment and theory *Surf. Sci. Rep.* **34** 171–294
[14] Ibach H 2006 *Physics of Surfaces and Interfaces* (Berlin: Springer)
[15] Einstein T 2007 Using the Wigner–Ibach surmise to analyze terrace-width distributions: history, user's guide, and advances *Appl. Phys.* A **87** 375–84
[16] Giesen M, Steimer C and Ibach H 2001 What does one learn from equilibrium shapes of two-dimensional islands on surfaces? *Surf. Sci.* **471** 80–100
[17] Davis S and Somorjai G 1980 The effect of surface oxygen on hydrocarbon reactions catalyzed by platinum crystal surfaces with variable kink concentrations *Surf. Sci.* **91** 73–91
[18] Besocke K, Krahl-Urban B and Wagner H 1977 Dipole moments associated with edge atoms; a comparative study on stepped Pt, Au and W surfaces *Surf. Sci.* **68** 39–46
[19] Morgenstern K, Braun K-F and Rieder K-H 2002 Surface-state depopulation on small Ag(111) terraces *Phys. Rev. Lett.* **89** 226801
[20] Schiller F *et al* 2014 Metallic thin films on stepped surfaces: lateral scattering of quantum well states *New J. Phys.* **16** 123025
[21] Bertel E and Donath M 1995 *Electronic Surface and Interface States on Metallic Systems: Proc. 134th WE-Heraeus Seminar (Physikzentrum, Bad Honnef, Germany, 17–20 October 1994)* (Singapore: World Scientific) p 63
[22] Bürgi L, Jeandupeux O, Hirstein A, Brune H and Kern K 1998 Confinement of surface state electrons in Fabry–Pérot resonators *Phys. Rev. Lett.* **81** 5370–3
[23] Morgenstern K, Rieder K-H and Fiete G A 2005 Disorder-induced local-density-of-states oscillations on narrow Ag(111) terraces *Phys. Rev.* B **71** 155413
[24] Hansmann M, Pascual J I, Ceballos G, Rust H-P and Horn K 2003 Scanning tunneling spectroscopy study of Cu(554): confinement and dimensionality at a stepped surface *Phys. Rev.* B **67** 121409
[25] Baumberger F, Hengsberger M, Muntwiler M, Shi M, Krempasky J, Patthey L, Osterwalder J and Greber T 2004 Localization of surface states in disordered step lattices *Phys. Rev. Lett.* **92** 196805
[26] Smoluchowski R 1941 Anisotropy of the electronic work function of metals *Phys. Rev.* **60** 661–74
[27] Wandelt K 1990 *Chemistry and Physics of Solid Surfaces VIII* ed R Vanselow and R Howe (Berlin: Springer) pp 289–334
[28] Neuhold G and Horn K 1997 Depopulation of the Ag(111) surface state assigned to strain in epitaxial films *Phys. Rev. Lett.* **78** 1327–30
[29] Bertel E 1995 One- and two-dimensional surface states on metals *Surf. Sci.* **331-333** 1136–46